

RESEARCH ARTICLE

# BMN 250, a fusion of lysosomal alpha-N-acetylglucosaminidase with IGF2, exhibits different patterns of cellular uptake into critical cell types of Sanfilippo syndrome B disease pathogenesis

Gouri Yogalingam <sup>\*</sup>, Amanda R. Luu, Heather Prill, Melanie J. Lo, Bryan Yip, John Holtzinger, Terri Christianson, Mika Aoyagi-Scharber, Roger Lawrence, Brett E. Crawford , Jonathan H. LeBowitz

Research, BioMarin Pharmaceutical, Inc., Novato, CA, United States of America

\* [gyogalingam@bmrn.com](mailto:gyogalingam@bmrn.com)



 OPEN ACCESS

**Citation:** Yogalingam G, Luu AR, Prill H, Lo MJ, Yip B, Holtzinger J, et al. (2019) BMN 250, a fusion of lysosomal alpha-N-acetylglucosaminidase with IGF2, exhibits different patterns of cellular uptake into critical cell types of Sanfilippo syndrome B disease pathogenesis. *PLoS ONE* 14(1): e0207836. <https://doi.org/10.1371/journal.pone.0207836>

**Editor:** Andrea Dardis, Azienda Ospedaliero-Universitaria Santa Maria della Misericordia, ITALY

**Received:** November 1, 2018

**Accepted:** December 19, 2018

**Published:** January 18, 2019

**Copyright:** © 2019 Yogalingam et al. This is an open access article distributed under the terms of the [Creative Commons Attribution License](https://creativecommons.org/licenses/by/4.0/), which permits unrestricted use, distribution, and reproduction in any medium, provided the original author and source are credited.

**Data Availability Statement:** All relevant data are within the paper and its Supporting Information files.

**Funding:** All authors are full time employees of BioMarin Pharmaceutical Inc. The funder provided support in the form of salaries for all authors, but did not have any additional role in the study design, data collection and analysis, decision to publish, or preparation of the manuscript. The specific roles of

## Abstract

Sanfilippo syndrome type B (Sanfilippo B; Mucopolysaccharidosis type IIIB) occurs due to genetic deficiency of lysosomal alpha-N-acetylglucosaminidase (NAGLU) and subsequent lysosomal accumulation of heparan sulfate (HS), which coincides with devastating neurodegenerative disease. Because NAGLU expressed in Chinese hamster ovary cells is not mannose-6-phosphorylated, we developed an insulin-like growth factor 2 (IGF2)-tagged NAGLU molecule (BMN 250; tralesenin alfa) that binds avidly to the IGF2 / cation-independent mannose 6-phosphate receptor (CI-MPR) for glycosylation independent lysosomal targeting. BMN 250 is currently being developed as an investigational enzyme replacement therapy for Sanfilippo B. Here we distinguish two cellular uptake mechanisms by which BMN 250 is targeted to lysosomes. In normal rodent-derived neurons and astrocytes, the majority of BMN250 uptake over 24 hours reaches saturation, which can be competitively inhibited with IGF2, suggestive of CI-MPR-mediated uptake.  $K_{\text{uptake}}$ , defined as the concentration of enzyme at half-maximal uptake, is 5 nM and 3 nM in neurons and astrocytes, with a maximal uptake capacity ( $V_{\text{max}}$ ) corresponding to 764 nmol/hr/mg and 5380 nmol/hr/mg, respectively. Similar to neurons and astrocytes, BMN 250 uptake in Sanfilippo B patient fibroblasts is predominantly CI-MPR-mediated, resulting in augmentation of NAGLU activity with doses of enzyme that fall well below the  $K_{\text{uptake}}$  (5 nM), which are sufficient to prevent HS accumulation. In contrast, uptake of the untagged recombinant human NAGLU (rhNAGLU) enzyme in neurons, astrocytes and fibroblasts is negligible at the same doses tested. In microglia, receptor-independent uptake, defined as enzyme uptake resistant to competition with excess IGF2, results in appreciable lysosomal delivery of BMN 250 and rhNAGLU ( $V_{\text{max}}$  = 12,336 nmol/hr/mg and 5469 nmol/hr/mg, respectively). These results suggest that while receptor-independent mechanisms exist for lysosomal targeting of rhNAGLU in microglia, BMN 250, by its IGF2 tag moiety, confers increased CI-MPR-mediated lysosomal targeting

these authors are articulated in the 'author contributions' section.

**Competing interests:** All authors are full time employees of BioMarin Pharmaceutical Inc. This does not alter our adherence to PLOS ONE policies on sharing data and materials. Mika Aoyagi-Scharber, Terri M. Christianson and Jonathan H. LeBowitz, together with others, are inventors on a patent claiming compositions and methods for treating Sanfilippo type B, comprising therapeutic NAGLU-IGF2 fusion proteins (US 9,376,480 B2).

**Abbreviations:** MPS, Mucopolysaccharidosis; NAGLU, alpha-N-acetylglucosaminidase; rhNAGLU, recombinant human NAGLU or tralesenidase alfa; IGF2, insulin-like growth factor 2; ERT, enzyme replacement therapy; CHO, Chinese hamster ovary; HS, heparan sulfate; HSPG, heparan sulfate proteoglycan; Man6P/M6P, mannose-6-phosphate; CI-MPR, cation-independent mannose 6-phosphate receptor; GILT, glycosylation independent lysosomal targeting.

to neurons and astrocytes, two additional critical cell types of Sanfilippo B disease pathogenesis.

## Introduction

Heparan sulfate (HS)–containing proteoglycans in the extracellular matrix and at the cell surface play important roles in the regulation of protease activity, growth factor signaling and cell surface receptor-mediated endocytosis of various ligands [1–2]. While little is understood regarding how these macromolecules contribute to disease one clue to their biological importance lies in a devastating group of inherited diseases involving impaired turnover of HS in lysosomes. Mucopolysaccharidosis III (MPS III; Sanfilippo syndrome) includes four biochemically distinct lysosomal storage diseases, each characterized by deficiency of a lysosomal enzyme involved in the step-wise degradation of HS [3]. Sanfilippo B exhibits an autosomal recessive mode of inheritance and arises from mutations in the *NAGLU* gene, which encodes alpha-N-acetylglucosaminidase (NAGLU). In its severest form Sanfilippo B patients exhibit non-detectable or very low levels of NAGLU activity in their lysosomes, which coincides with lysosomal HS accumulation in the brain and ultimately leads to severe neurodegenerative disease and early death [4–5]. However, little is understood regarding the mechanism by which accumulation of HS in lysosomes leads to neurodegenerative disease in Sanfilippo syndrome. Studies in a mouse model of Sanfilippo B suggest that neurons and astrocytes of the Sanfilippo B brain may be compromised as a consequence of elevated levels of HS [6–7]. HS accumulation in microglia is also thought to contribute to neurodegeneration associated with Sanfilippo B [8–9]. Developing therapeutic approaches to augment NAGLU activity in these critical cell types of neurodegenerative disease pathogenesis in Sanfilippo B may therefore be paramount for successful clearance of accumulated substrate, subsequently leading to correction of underlying pathology and stabilization of the disease.

In most cases of Sanfilippo B and other MPS disorders, the entire range of clinical phenotypes ranging from severe to relatively mild are clustered within a narrow range of residual lysosomal enzyme activity, from 0–20% of normal control levels [10–13]. These genotype-phenotype correlations suggest that reduced levels of residual lysosomal enzyme activity, down to a critical “threshold”, are sufficient to turn over substrate *in vivo* and prevent lysosomal storage disease and that small changes in residual activity below this threshold may lead to dramatic differences in the rate of substrate turn-over and the severity of the lysosomal storage disease [14]. This, in turn, implies that enzyme activity does not need to be normalized to prevent lysosomal storage of substrate in MPS patient cells to attenuate their disease progression and that only very small increases in residual enzyme activity may be sufficient. Several approved products for MPS have exploited this phenomenon to develop lysosomal-targeted enzyme replacement therapies (ERT) to augment residual lysosomal enzyme activity in patients, resulting in substrate reduction and improved quality of life [15]. These ERT trials have utilized the cell surface insulin-like growth factor 2 (IGF2) / cation-independent mannose-6-phosphate receptor (CI-MPR) targeting pathway, where phosphorylated glycans present on secreted lysosomal enzymes bind avidly to the CI-MPR, resulting in their internalization into clathrin-coated vesicles, and delivery to lysosomes of patient cells [16].

In the case of ERT development for Sanfilippo B, recombinant human NAGLU (rhNAGLU) over-expressed and secreted in Chinese hamster ovary (CHO) cells and in Sanfilippo B human fibroblasts is not mannose -6-phosphorylated [17,10], a property that may severely

limit its uptake into key critical cellular targets of disease pathogenesis. Our group has therefore utilized a glycosylation independent lysosomal targeting (GILT) system, whereby IGF2 has been fused to rhNAGLU (rhNAGLU-IGF2; BMN 250) to mediate CI-MPR-mediated cellular uptake and delivery to lysosomes [18–20]. BMN 250 is a novel recombinant fusion protein currently being developed as an investigational ERT for Sanfilippo B. We have shown that intracerebroventricular (ICV) administration of BMN 250 in a knock-out mouse model and a naturally occurring dog model of Sanfilippo B can augment NAGLU activity and NAGLU protein levels in all cell types throughout the brain, normalize HS levels and reverse several aspects of well-entrenched secondary neuropathology associated with the disease [20–22]. While normalization of HS levels in the Sanfilippo B mouse and dog brains with ICV-administered BMN 250 is indicative of successful enzyme delivery to critical cellular targets of Sanfilippo B disease pathogenesis, the cellular uptake mechanism/s by which this process occurs in critical cell types of the brain has yet to be demonstrated.

Here we performed a series of competitive cellular uptake assays with BMN 250 in primary human Sanfilippo B patient fibroblasts and normal rodent-derived neurons, astrocytes and microglia. These studies distinguish two pathways by which BMN 250 in the extracellular space can be delivered to lysosomes of cells to augment residual NAGLU activity. We demonstrate that GILT technology confers predominantly CI-MPR-mediated cellular uptake and delivery of BMN 250 to lysosomes in neurons, astrocytes and fibroblasts, whereas receptor-independent cellular uptake in microglia contributes to substantial lysosomal delivery of both BMN 250 and untagged rhNAGLU. We also developed an assay in Sanfilippo B patient fibroblasts to mimic the limited and transient exposure of BMN 250 to critical cells types of disease pathogenesis in the Sanfilippo B brain following ICV administration. Our results suggest that a minimum threshold of ~20% of wild-type residual NAGLU activity levels is required to completely prevent accumulation of HS in Sanfilippo B patient fibroblasts and that only BMN 250 cellular uptake under very limiting and transient exposure conditions occurs in sufficient amounts to reach this threshold.

## Results and discussion

### BMN 250 uptake is predominantly CI-MPR-mediated in mouse hippocampal neurons

In normal mouse-derived hippocampal neurons, the majority of BMN250 uptake over 24 hours approximates Michaelis-Menten kinetics with a  $K_{\text{uptake}}$  of 5 nM (Fig 1A and Table A in S1 File). AF-488-tagged BMN 250 co-localizes with LysoTracker Red<sup>+</sup> acidified organelles in the cell body and along axonal projections of mouse neuronal hippocampal cells following cellular uptake, suggestive of successful delivery to lysosomes (Fig 1C, 1D and 1E). At the highest BMN 250 concentration tested (100 nM) NAGLU activity is increased by 13-fold, when compared with endogenous NAGLU activity detected in normal untreated mouse hippocampal neurons (Fig 1B and Table B in S1 File). Furthermore, at this highest dose tested (100 nM) the majority of BMN 250 uptake in mouse hippocampal-derived neurons is inhibited in the presence of 4  $\mu$ M IGF2, a competitive inhibitor of CI-MPR-mediated cellular uptake, suggesting that the majority of BMN 250 cellular uptake is CI-MPR-mediated (Fig 1B and Table B in S1 File). CI-MPR-independent BMN 250 cellular uptake in mouse hippocampal neurons is sufficient to augment NAGLU activity by 2.5-fold, when compared with endogenous NAGLU activity detected in untreated normal mouse hippocampal neurons (Fig 1B). The untagged rhNAGLU is also taken up into mouse hippocampal neurons at the highest nM concentration tested (100 nM), which is sufficient to augment NAGLU activity by 2.1-fold above normal levels in untreated normal hippocampal neurons (Fig 1B). Glycan analysis of CHO-expressed

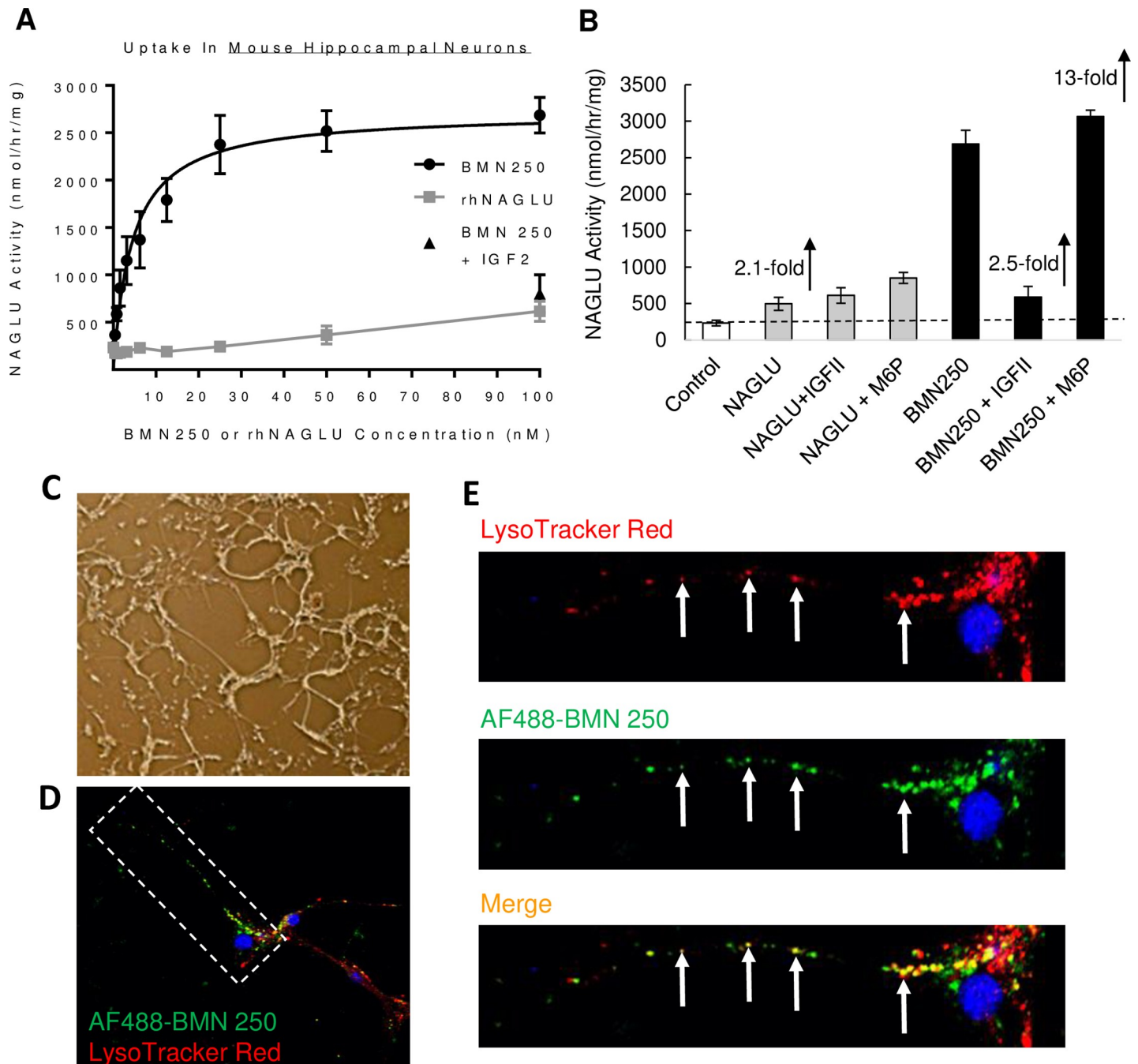


**Fig 1. BMN 250 is delivered to lysosomes of mouse-derived hippocampal axonal projections.** A, NAGLU activity detected in triplicate cultures of mouse hippocampal neurons following uptake of BMN 250 and rhNAGLU over 24 hours. BMN 250 Kuptake = 4.5 nM; Vmax = 2716 nmol/hr/mg. rhNAGLU Kuptake = 5.2 nM; Vmax = 447 nmol/hr/mg B, NAGLU activity levels detected following uptake of rhNAGLU or BMN 250 in the absence or presence of 4  $\mu$ M IGF2 or 5 mM M6P, as indicated. The level of endogenous NAGLU activity detected in normal mouse hippocampal neurons is indicated with a hashed line. C, Representative phase-contrast image of cells described (B) following uptake with BMN 250; D, Merged confocal image of a single neuron incubated with AF488 BMN 250 and LysoTracker Red. E, Expanded images of the axonal projection highlighted in D. Arrows represent examples of AF488 BMN 250 co-localization with LysoTracker Red+ organelles in the merged image. Data sets for panel A and B are shown in the supporting information.

<https://doi.org/10.1371/journal.pone.0207836.g001>

NAGLU-IGF2 and untagged rhNAGLU molecules have previously demonstrated the absence of phosphorylated glycans [20]. In support of this the addition of Man6P to the uptake

medium does not inhibit uptake of rhNAGLU or BMN 250 (Fig 1B). These results suggest BMN 250 uptake is predominantly CI-MPR-mediated in mouse hippocampal-derived neurons, with receptor-independent uptake only becoming apparent at higher concentrations.

### **BMN 250 uptake into rat neurons and astrocytes is predominantly ci-mpr-mediated, whereas uptake in rat microglia occurs through ci-mpr-mediated and receptor-independent mechanisms**

BMN 250 cellular uptake was also evaluated in primary rat-derived neurons, astrocytes and microglia to permit comparison between three different cell types from the same species. NAGLU activity, standardized to total protein levels in each normal rat-derived cell line varies considerably, with comparatively higher levels of NAGLU activity being detected in normal rat-derived microglia ( $1120 \pm 341$  nmol/hr/mg), when compared with normal rat-derived cortical neurons ( $93 \pm 24$  nmol/hr/mg) and astrocytes ( $166 \pm 5$  nmol/hr/mg; Fig 2A). A low-dose exposure to 6.25 nM BMN 250 over 24 hours results in highly efficient cellular uptake of BMN 250 in all three primary rat cell lines, with 5-fold, 25-fold and 14-fold increases in NAGLU activity above normal endogenous NAGLU activity levels detected in untreated rat neurons, astrocytes and microglia, respectively (Fig 2B, 2C and 2D and Table C in S1 File). In contrast, NAGLU can only be detected in rat microglia following a 24 hour exposure to a low nM dose (6.25 nM) of the untagged rhNAGLU. Furthermore, the NAGLU activity that was detected in rat microglia following exposure to a low nM dose of untagged rhNAGLU was increased by 2.5-fold over endogenous NAGLU activity detected in normal rat microglia (Fig 2D). No NAGLU activity was detected in rat derived cortical neurons and astrocytes following a 24 hour exposure to a low nM dose (6.25 nM) of untagged rhNAGLU (Fig 2B and 2C, respectively). The lack of detectable rhNAGLU uptake in rat cortical neurons (Fig 2B) contrast with our rhNAGLU uptake results in mouse hippocampal neurons, where some uptake was observed (Fig 1B). While we did not study the mechanism of CI-MPR-independent rhNAGLU uptake into mouse hippocampal neurons, it remains possible that this process is occurring in a neuronal sub-population-specific and / or a species-specific manner. Collectively, these results suggest that of the three primary cell rat lines tested, BMN 250 can normalize NAGLU activity in all three cell lines at low nM concentrations, whereas untagged rhNAGLU can only normalize NAGLU activity in microglia.

To determine the enzyme uptake capacity ( $V_{\max}$ ) for each rat-derived cell line a series of uptake curves were performed with increasing doses of BMN 250 or untagged rhNAGLU. As previously shown in ICV-ERT studies in Sanfilippo B mice [21], of the three rat-derived primary cell type cultures tested, untagged rhNAGLU only shows appreciable uptake in microglial cells, with low or non-detectable uptake detected in cortical neurons and astrocytes (Fig 3A and Table D in S1 File). In contrast, BMN 250 uptake can be readily detected in all three cell types over a 24 hour period (Fig 3B and Table E in S1 File), with  $K_{\text{uptake}}$  corresponding to 5 nM in cortical neurons, 3.4 nM in astrocytes and 2.6 nM in microglia (Fig 3B). These results are in agreement with our previous *in vivo* studies, with NAGLU protein being detected in neurons, astrocytes and microglia of the Sanfilippo B mouse brain following ICV administration of BMN 250 [21].

BMN 250 uptake capacity in microglia ( $V_{\max} = 12,383$  nmol/hr/mg; Fig 3B) exceeds the uptake capacity reached in cortical neurons ( $V_{\max} = 1,055$  nmol/hr/mg; Fig 3B) and astrocytes ( $V_{\max} = 5,404$  nmol/hr/mg; Fig 3B). The majority of BMN 250 uptake into rat cortical neurons and astrocytes is blocked with the addition of 4  $\mu$ M IGF2 to the uptake medium, (Fig 4A and 4B, Table F and G in S1 File), suggesting that BMN 250 uptake and delivery to lysosomes is predominantly CI-MPR-mediated. In contrast to rat neurons and rat astrocytes, rat microglia

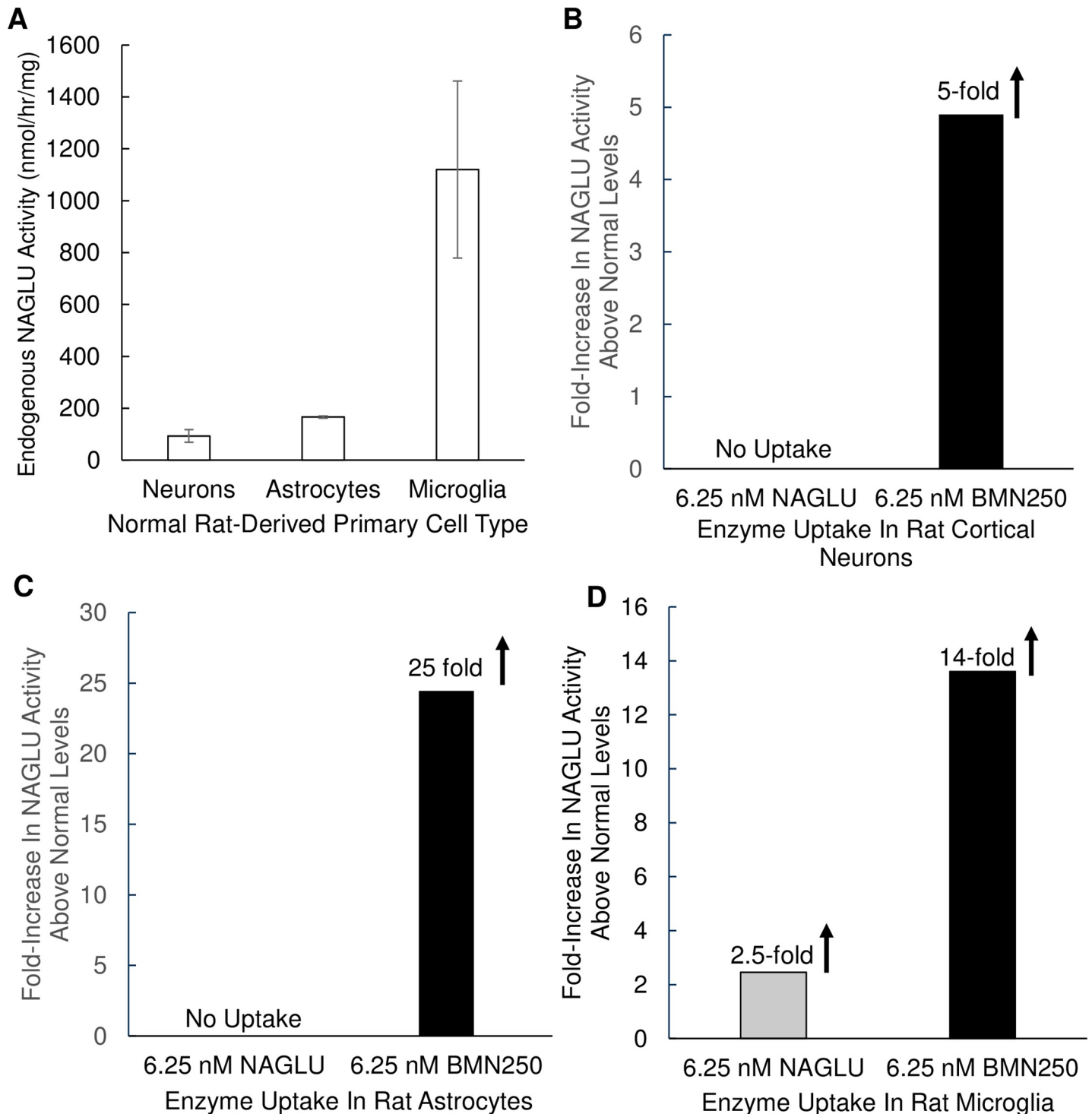


**Fig 2. Evaluation of BMN 250 and rhNAGLU uptake in normal rat neurons, astrocytes and microglia.** A. Endogenous NAGLU activity levels present in normal rat-derived primary cortical neurons, astrocytes and microglia. To permit comparison between cell lines NAGLU activity levels present in cell lysates prepared from three separate cultures of each cell type was standardized to total protein levels and expressed as nmol/hr/mg total cell protein. Results are expressed as the mean (N = 3) ± SD. B, C, D. NAGLU activity levels present in normal rat-derived primary cultures of cortical neurons (A), astrocytes (B) and microglia (C) following 24 hours of cellular uptake with 6.25 nM BMN 250 (black bars) or 6.25 nM rhNAGLU (grey bars). NAGLU activity is presented as the fold-increase above normal endogenous levels of NAGLU activity in each cell line. Data sets for Fig 2 are shown in the Supporting information.

<https://doi.org/10.1371/journal.pone.0207836.g002>

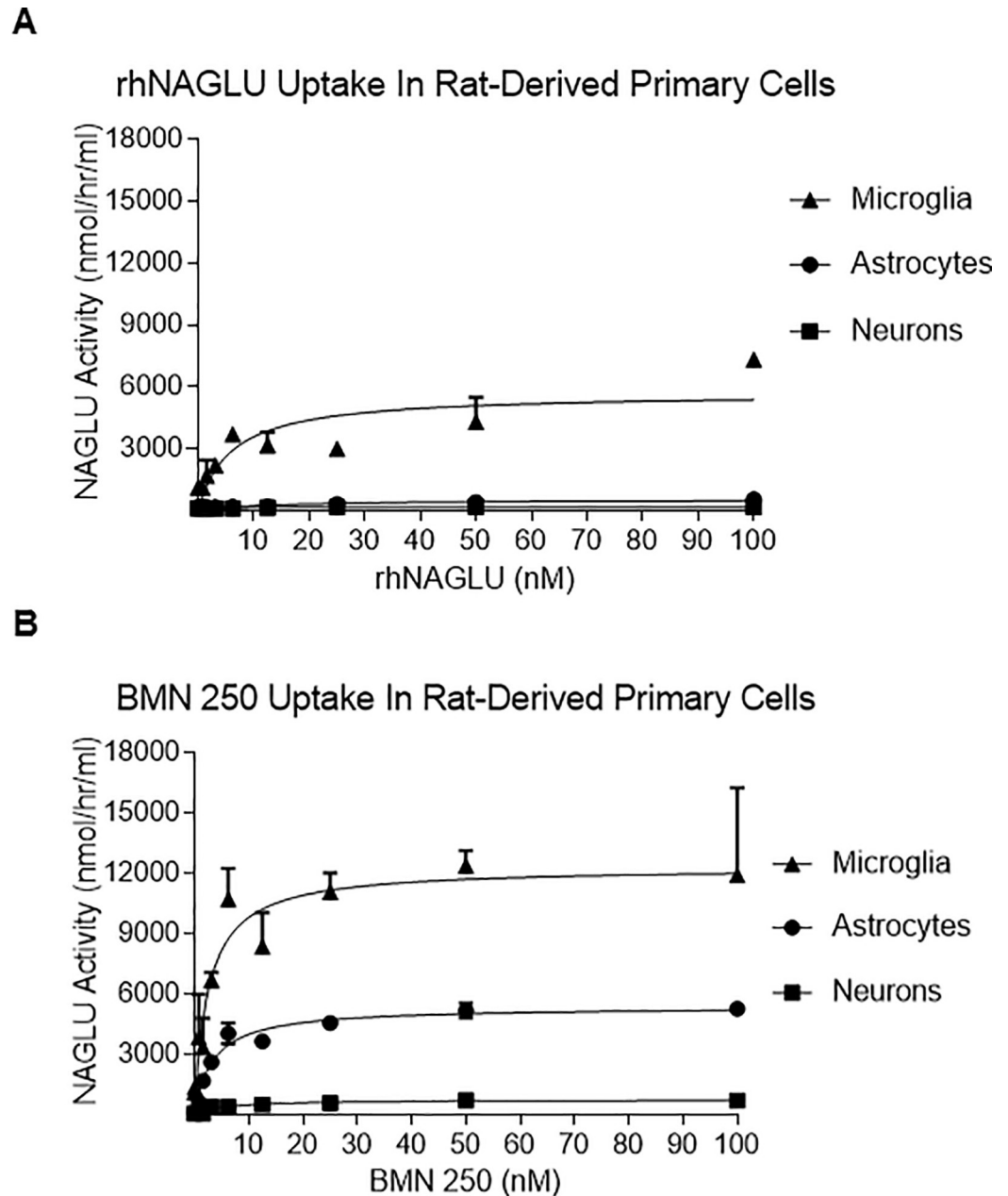


**Fig 3. BMN 250 and rhNAGLU exhibit differential uptake capacities in normal rat-derived neurons, astrocytes and microglia.** A, B: Representative curves of rhNAGLU uptake (A) or BMN 250 uptake (B) over 24 hours in duplicate cultures of normal rat-derived primary cultures of cortical neurons (squares), astrocytes (circles) and microglia (triangles). rhNAGLU kuptake in microglia = 4.7 nM; rhNAGLU Vmax in cortical neurons = 179 nmol/hr/mg, astrocytes = 371 nmol/hr/mg, microglia = 5469 nmol/hr/mg. BMN 250 Kuptake in cortical neurons = 5.05 nM, astrocytes = 3.4 nM, microglia = 2.6 nM. BMN 250 Vmax in cortical neurons = 764 nmol/hr/mg, astrocytes = 5380 nmol/hr/mg, microglia = 12,312 nmol/hr/mg. Data sets for Fig 3 are shown in the supporting information section.

<https://doi.org/10.1371/journal.pone.0207836.g003>

appear to possess an efficient CI-MPR-independent uptake pathway, since the addition of 4  $\mu$ M IGF2 to the uptake medium only partially inhibits the uptake of BMN 250 into rat microglia (Fig 4C and Table H in S1 File). CI-MPR-dependent uptake into microglia, plotted against enzyme concentration approximates Michaelis-Menten kinetics, with a  $K_{\text{uptake}}$  of 2.2 nM (Fig

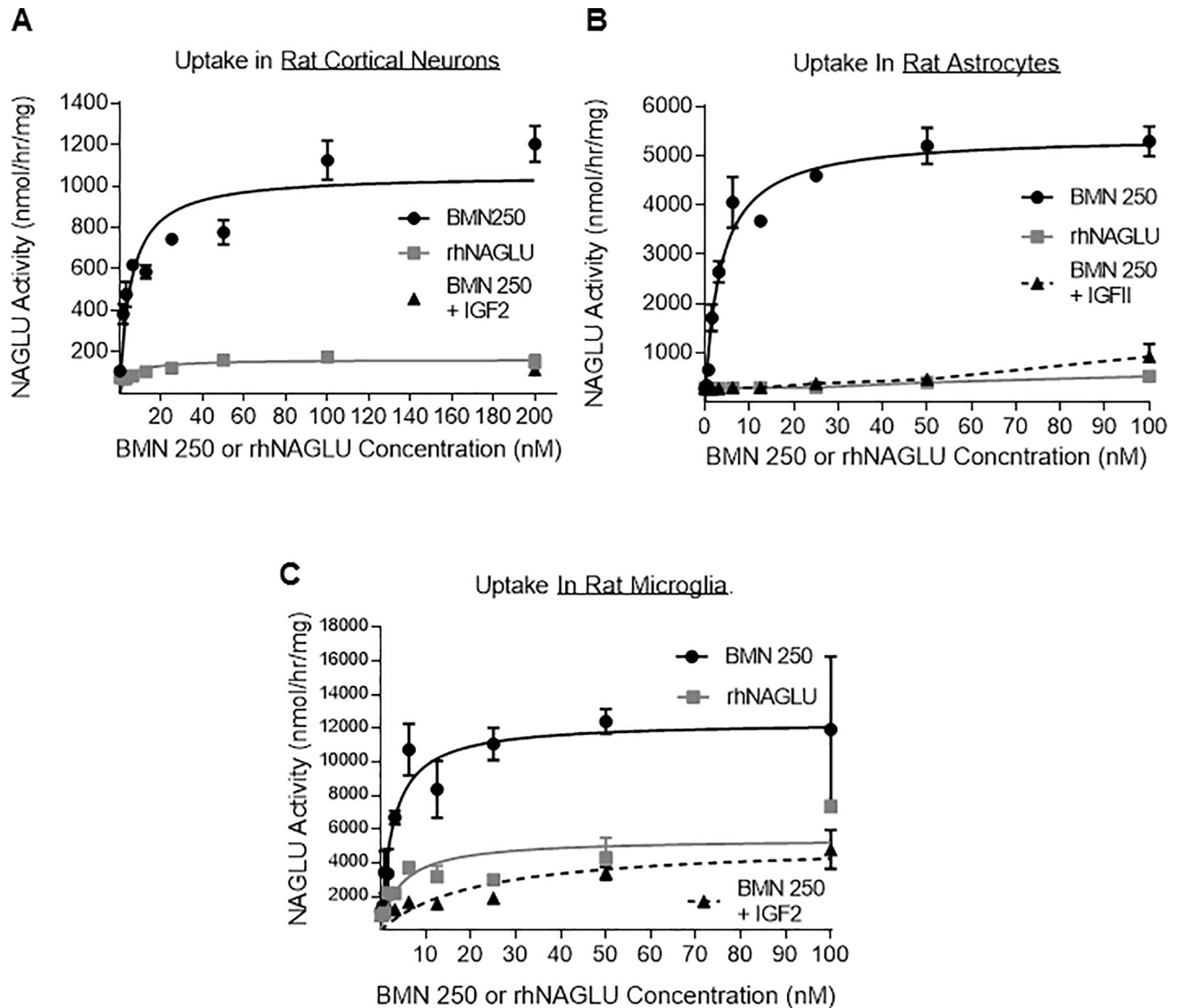
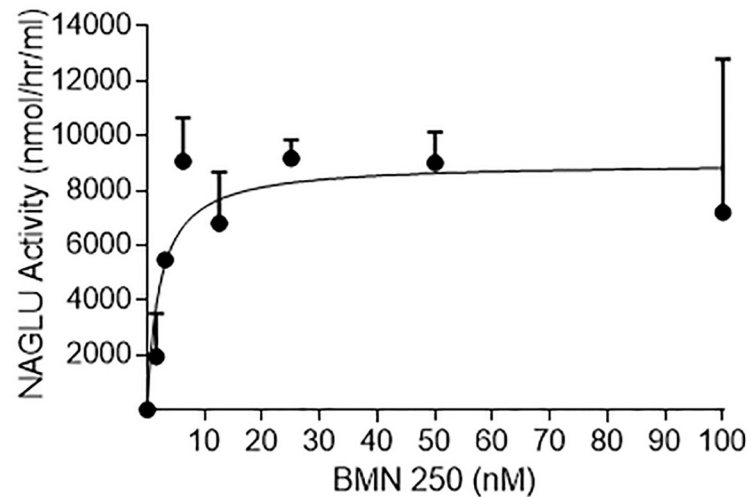


**Fig 4. BMN 250 exhibits CI-MPR-dependent and receptor-independent uptake in rat-derived neurons, astrocytes and microglia.** A, B and C: Representative uptake curves of BMN 250 in the absence (black circles) or presence (grey squares) of 4  $\mu$ M IGF2, or rhNAGLU (black triangles, hashed line) as indicated, in duplicate cultures of normal rat-derived primary cultures of cortical neurons (A; N = 1 repeat) astrocytes (B; N = 3 repeats) and microglia (C; N = 3 repeats). BMN 250 Kuptake in rat cortical neurons = 5.0 nM,  $V_{max}$  = 1,055 nmol/hr/mg; BMN 250 Kuptake in astrocytes = 3.4 nM,  $V_{max}$  = 5,404 nmol/hr/mg; BMN 250 Kuptake in microglia = 2.6 nM,  $V_{max}$  = 12,383 nmol/hr/mg; BMN 250 Kuptake in microglia in the presence of 4  $\mu$ M IGF2 = 21.4 nM,  $V_{max}$  = 5148 nmol/hr/mg; rhNAGLU Kuptake in microglia = 4.5 nM;  $V_{max}$  = 5424 nmol/hr/mg. Data sets for Fig 4 are shown in the supporting information section.

<https://doi.org/10.1371/journal.pone.0207836.g004>

5A and Table I in S1 File). In contrast, receptor-independent uptake of BMN 250 in microglia plotted against enzyme concentration shows that the pattern of enzyme uptake does not reach saturation, suggestive of receptor-independent uptake (Fig 5B and Table J in S1 File). Likewise, cellular uptake of the untagged rhNAGLU in rat microglia is also observed (Fig 4C), which contrasts with rhNAGLU uptake in rat neurons and astrocytes (Fig 4A and 4B). These results are suggestive of both CI-MPR-mediated and receptor-independent mechanisms being

**A**  
**CI-MPR-Dependent  
 BMN 250 Uptake In Rat-Derived Microglia**



**B**  
**Receptor-Independent  
 BMN 250 Uptake In Rat-Derived Microglia**

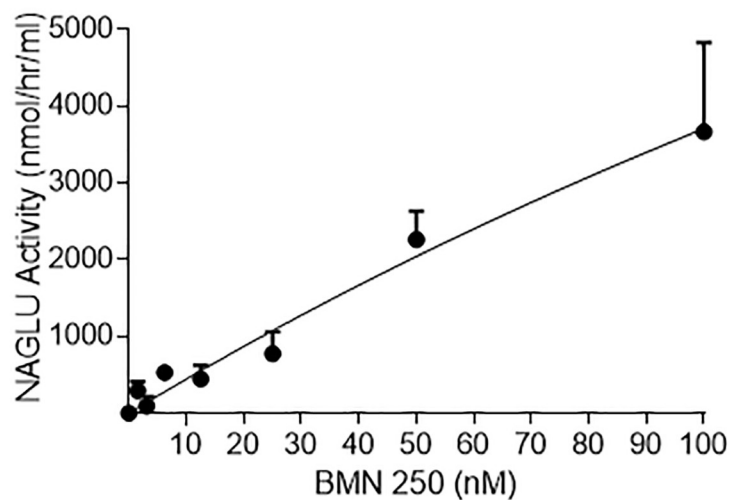


**Fig 5. Evaluation of CI-MPR-Dependent and Receptor-Independent BMN 250 Uptake In Rat-Derived Neurons, Astrocytes And Microglia.** A, CI-MPR-dependent uptake of BMN 250 in duplicate cultures of rat microglia was calculated by subtracting endogenous NAGLU activity and the uptake achieved in the presence of 4  $\mu$ M IGF2 from the total amount of uptake achieved with BMN250 in the absence of inhibitor. BMN 250 Kuptake in microglia = 2.2 nM,  $V_{max}$  = 9,009 nmol/hr/mg B, Receptor-Independent uptake of BMN 250 achieved in the presence of 4  $\mu$ M IGF2 in microglia was calculated by subtracting endogenous NAGLU activity detected in untreated microglia. N = 3 repeats. Data sets for Fig 5 are shown in the supporting information section.

<https://doi.org/10.1371/journal.pone.0207836.g005>

utilized in the cellular uptake and lysosomal targeting of BMN 250 in rat-derived neurons, astrocytes and microglia, with the highest levels of receptor-independent uptake occurring in microglia.

### BMN 250 uptake in Sanfilippo B patient fibroblasts is predominantly ci-mpr-mediated and is sufficient to prevent hs accumulation

Our results in primary neurons, astrocytes and microglia are suggestive of BMN 250 cellular uptake and delivery to lysosomes being mediated by both CI-MPR-mediated and receptor-independent mechanisms to varying degrees, depending on the enzyme concentration and the cell type. To further understand the therapeutic relevance of CI-MPR-mediated BMN 250 uptake we utilized Sanfilippo B patient fibroblasts that are known to accumulate HS [23]. Similar to the uptake pattern observed in neurons and astrocytes, BMN 250 uptake in Sanfilippo B patient fibroblasts over 24 hours approximates Michaelis-Menten kinetics with a  $K_{\text{uptake}}$  of 5.1 nM and is predominantly CI-MPR-mediated, since the majority of uptake can be inhibited with IGF2 (Fig 6 and Table K in S1 File). Receptor independent uptake is observed at the higher concentrations and is similar to uptake of untagged rhNAGLU (Fig 6).

We next developed an assay in Sanfilippo B patient fibroblasts to mimic the limited and transient exposure of BMN 250 to critical cells types of disease pathogenesis in the Sanfilippo B brain. Incubation of Sanfilippo B patient fibroblasts with concentrations of BMN 250 at or below the 5.1 nM  $K_{\text{uptake}}$  (1.56, 3.125 or 6.25 nM BMN 250) for 2 hours, followed by a further 8 days of culture results in dose-dependent increases in NAGLU activity, corresponding to 8%, 16% and 21% of normal NAGLU activity levels detected in fibroblasts from a healthy control individual, respectively (Fig 7A and Table L in S1 File). BMN 250 uptake coincides with dose-dependent reduction in the amount of HS accumulation (Fig 7A). At the highest

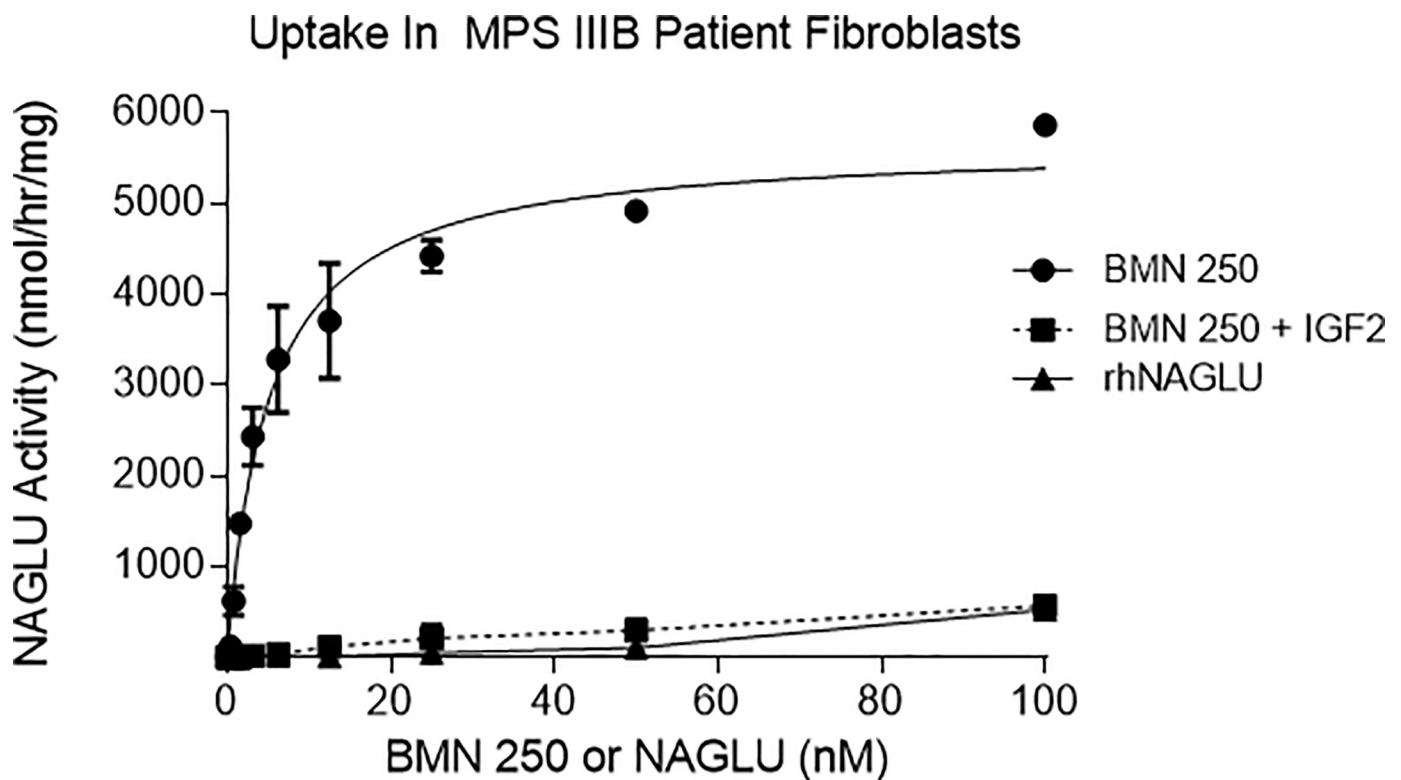


**Fig 6. BMN 250 exhibits CI-MPR-dependent and receptor-independent uptake in Sanfilippo syndrome B patient fibroblasts.** Representative uptake curves of BMN 250 in duplicate cultures of MPS IIIB patient fibroblasts in the absence (black circles) or presence (black squares) of 4  $\mu$ M IGF2, or rhNAGLU (black triangles), as indicated. BMN 250  $K_{\text{uptake}}$  = 5.1 nM; BMN 250  $V_{\text{max}}$  = 5663 nmol/hr/mg. No NAGLU activity was detected in control untreated cells. N = 3 repeats. The complete data set for this figure is shown in the supporting information section.

<https://doi.org/10.1371/journal.pone.0207836.g006>

concentration of BMN 250 tested (6.25 nM), HS accumulation is completely prevented, suggestive of successful delivery of BMN 250 to lysosomes of Sanfilippo B patient fibroblasts (Fig 7A). In support of this AF488-labeled BMN 250 co-localizes with LysoTracker Red<sup>+</sup> organelles following cellular uptake in Sanfilippo B patient fibroblasts (Fig 7C). Collectively, these results suggest that under conditions of limited and transient exposure, cellular uptake of BMN 250 is sufficient to partially restore NAGLU activity in Sanfilippo B patient cells. Furthermore, in line with genotype-phenotype correlations for various MPS diseases [10–13], our results suggest that only very small increases in residual NAGLU activity (~20% of normal NAGLU activity levels) are sufficient to completely prevent HS accumulation in Sanfilippo B patient cells (Fig 7A). In contrast to BMN 250, untagged rhNAGLU does not exhibit cellular uptake into

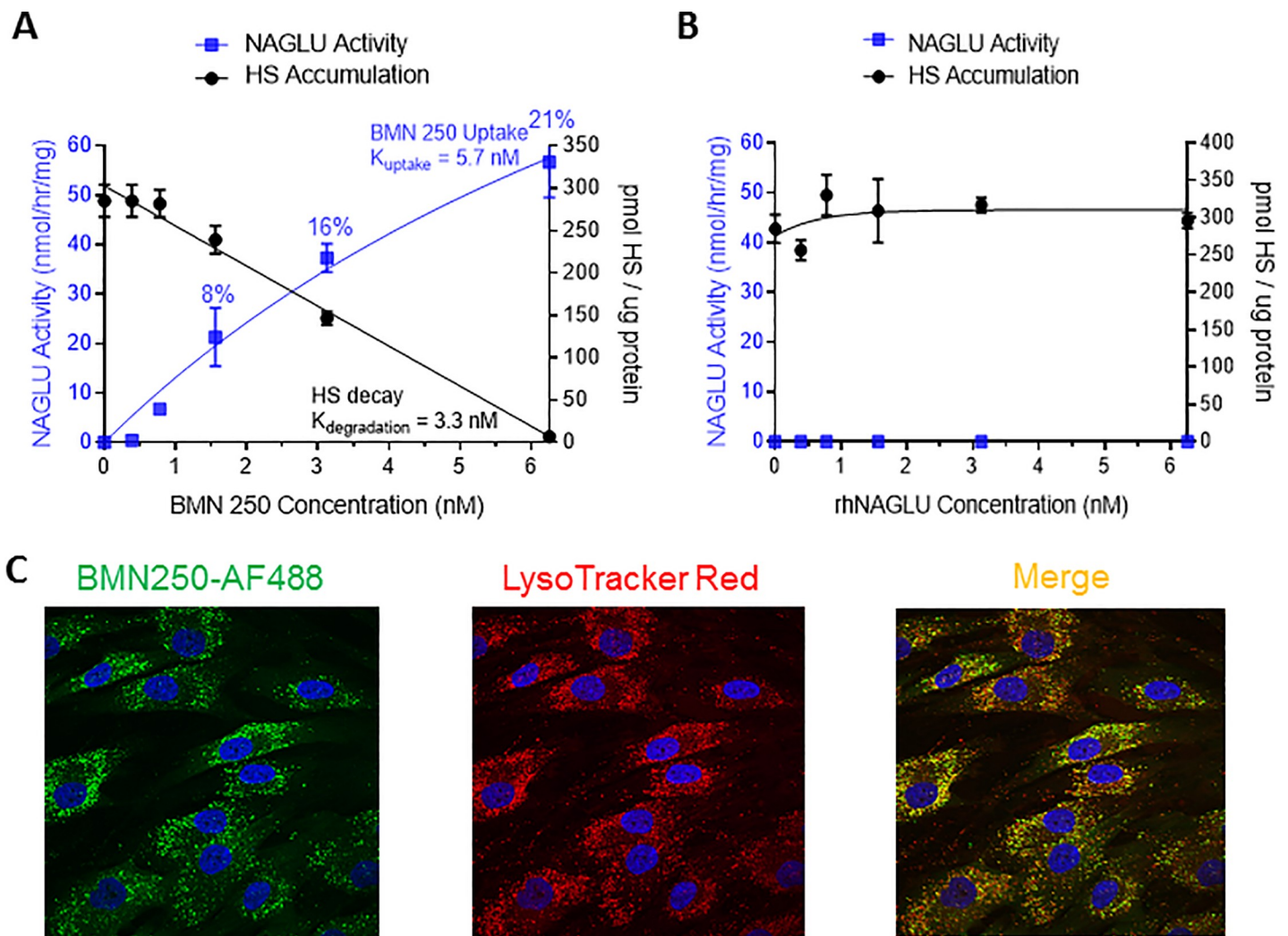


**Fig 7. BMN 250 uptake in Sanfilippo syndrome B patient fibroblasts under transient and limiting conditions is sufficient to prevent HS accumulation.** A, B, NAGLU activity present in MPS IIIB patient fibroblasts incubated with doses of BMN 250 equivalent to or below the BMN 250  $K_{\text{uptake}}$  (A; blue squares) or rhNAGLU (B; blue squares) for two hours on Day 2 of culture. Cells were washed extensively, then cultured for a further 8 days and analyzed for NAGLU activity using 4MU substrate. NAGLU activity detected is representative of three replicate cultures. Corresponding levels of HS detected at each enzyme concentration using SensiPro assay are indicated with black circles. NAGLU activity was augmented by 8%, 16% and 21% of normal NAGLU activity levels following incubation with 1.56 nM, 3.125, and 6.25 nM BMN 250, respectively, which coincides with dose-dependent clearance of HS. C. AF488-BMN 250 co-localizes with LysoTracker Red<sup>+</sup> lysosomes following uptake in Sanfilippo B patient fibroblasts. Data sets for panel A and B are shown in the supporting information section.

<https://doi.org/10.1371/journal.pone.0207836.g007>

Sanfilippo B patient fibroblasts under the same transient and limited exposure conditions, which coincides with no reduction in HS storage (Fig 7B and Table M in S1 File).

In conclusion, our results suggest that while untagged rhNAGLU exhibits efficient receptor-independent cellular uptake into microglia, negligible uptake of untagged rhNAGLU is observed in cultured neurons or astrocytes. BMN 250, an IGF2-tagged NAGLU molecule, overcomes this obstacle by permitting highly efficient CI-MPR-mediated cellular uptake and lysosomal delivery of NAGLU into neurons and astrocytes. Furthermore, only BMN 250 can augment residual NAGLU activity in Sanfilippo B patient fibroblasts in amounts that are sufficient to prevent HS accumulation under conditions of transient and limited enzyme exposure, a phenomenon which may potentially occur at sites of the Sanfilippo B brain that are distal to the site of ICV-administered enzyme. Studies in primary cultures of Sanfilippo B mouse-derived neurons and astrocytes further support these conclusions [23]. If clearance of HS from neurons and astrocytes throughout the brain is critical for treatment of Sanfilippo B, then an efficient targeting mechanism such as that possessed by BMN 250 will be critical for successful augmentation of NAGLU activity and effective treatment of this disease.

## Methods

### Cell lines

Human MPSIIIB fibroblasts (GM02931) were obtained from the Coriell Institute for Medical Research (Camden, NJ). GM02931 were grown and passaged in MEM supplemented with 15% fetal bovine serum (FBS; 15% v/v) and non-essential amino acids (Thermo Fisher Scientific, Waltham, M). Cortical neurons enriched from embryonic day 18 normal rat cerebrum were obtained from ScienCell Research Laboratories (Carlsbad, CA). Normal mouse-derived embryonic day 17 hippocampal neurons were obtained from Lonza Group Ltd. (Walkersville, MD). Astrocytes and microglia were enriched from post-natal day 2 normal rat total brain tissue were also obtained from ScienCell Research Laboratories (Carlsbad, CA). Neurons, astrocytes and microglia were cultured in poly-L-lysine-treated 96-well black tissue-culture-treated plates using defined medium, as recommended by the supplier.

### Direct “in-plate” NAGLU activity determination

NAGLU activity levels in cells plated in 96-well plates, as described above, was determined using the 4MU substrate, 4-Methylumbelliferyl-N-acetyl- $\alpha$ -D-glucosaminide. Briefly, cells in each well were washed extensively then lysed at room temperature for 15 minutes with 57.5  $\mu$ L of mammalian protein extraction reagent per well (M-PER; ThermoFisher Scientific, Waltham, MA). Of this lysate, 10  $\mu$ L was used to determine total protein levels using a BCA protein assay kit (ThermoFisher Scientific, Waltham, MA). The remaining lysate in each well was then incubated in the presence of 2 mM 4-Methylumbelliferyl-N-acetyl- $\alpha$ -D-glucosaminide in 0.2 M Acetate buffer pH 4.8 for 30 minutes at 37°C in a total reaction volume of 85  $\mu$ L. The reactions were terminated by addition of 200  $\mu$ L Glycine/NaOH buffer pH 10.7 to each well and plates were read at Ex360 Em460 with 455 cut off using a Spectramax i3 plate reader (Molecular Devices). A standard curve containing known amounts of 4-Methylumbelliferone (4-MU Standard; Sigma-Aldrich, St Louis, MO) was included in each assay to calculate NAGLU activity levels. In some instances where indicated, 4  $\mu$ M IGF2 (Cell Sciences, Canton, MA) or 5 mM mannose-6-phosphate (Man6P; Sigma-Aldrich, St Louis, MO) was added to uptake medium.

## Enzyme uptake studies

Recombinant human NAGLU-IGF2 fusion and NAGLU proteins were expressed in Chinese hamster ovary cells and purified, as described elsewhere (US 9,376,480 B2; Reference 20). To determine how much BMN 250 is required to normalize NAGLU activity, endogenous NAGLU activity in each normal primary neuron, astrocyte or microglia cell line was compared with BMN 250-specific NAGLU activity following a 24 hour exposure to 6.25 nM BMN 250 or 6.25 nM rhNAGLU in the presence of 4  $\mu$ M IGF2. Following BMN 250 uptake, cell lysates were prepared and assayed for NAGLU activity as described above. To determine the fold-increase above normal levels arising from BMN 250 uptake or rhNAGLU uptake, NAGLU activity following enzyme uptake was compared with the normal endogenous NAGLU activity level in each cell line.

## $K_{\text{uptake}}$ determination

To determine the  $K_{\text{uptake}}$ , the concentration of enzyme mediating half-maximal uptake, cells were incubated with varying concentrations of enzyme over a 24 hour period (dose-range 0.195 nM  $\rightarrow$  100), at which time the enzyme activity present in cells was plotted into a Michaelis-Menten curve using GraphPad Prism software (La Jolla, CA).

## Immunofluorescence

BMN 250 uptake in primary cells was also monitored by imaging, where BMN 250 was directly conjugated with Alexa Fluor 488 (AF488) prior to uptake. BMN 250 was conjugated to AF488 using a 5 fold-molar excess of AF488 Sulfodichlorophenol Ester (Thermo Scientific A30052) and purified as described by the manufacturer, yielding approximately 3 fluorophores per molecule of BMN 250. AF488 conjugation did not affect activity the activity of NAGLU toward 4MU substrate (Untagged BMN 250 specific activity = 3  $\mu$ mol/min/mg, versus AF488-conjugated BMN 250 specific activity = 2.8 nmol/min/mg). Cells were incubated with 0.2–0.4  $\mu$ M LysoTracker Red prior to fixation to permit identification of acidified lysosomes.

## Quantitative analysis of HS in MPSIIIB patient fibroblasts

Total heparan sulfate was quantified using a modification of the method previously described [24–25]. Total HS data is expressed as average pmoles total HS per  $\mu$ g total protein from triplicate sample wells per condition  $\pm$  SD.

## Supporting information

**S1 File.** Data sets used to generate data shown in paper (see [Results and Discussion](#) for details).  
(PPTX)

## Acknowledgments

We thank Gordon Vehar for his encouragement with initiating this exploratory project to support the BMN 250 program. Thanks also to Emma McCullagh for proof-reading the manuscript.

## Author Contributions

**Conceptualization:** John Holtzinger, Mika Aoyagi-Scharber, Jonathan H. LeBowitz.

**Data curation:** Gouri Yogalingam.

**Formal analysis:** Gouri Yogalingam.

**Investigation:** Gouri Yogalingam, Mika Aoyagi-Scharber.

**Methodology:** Amanda R. Luu, Heather Prill, Melanie J. Lo, Bryan Yip, John Holtzinger, Terri Christianson.

**Project administration:** Gouri Yogalingam, Mika Aoyagi-Scharber.

**Supervision:** Gouri Yogalingam, Terri Christianson, Roger Lawrence, Brett E. Crawford.

**Validation:** Gouri Yogalingam.

**Visualization:** Gouri Yogalingam.

**Writing – original draft:** Gouri Yogalingam.

**Writing – review & editing:** Gouri Yogalingam, Jonathan H. LeBowitz.

## References

1. Mulloy B. and Rider C.C. (2006) Cytokines and proteoglycans: an introductory overview. *Biochem Soc Trans* 34(3): 409–413
2. Christianson H.C. and Belting M. (2014) Heparan sulfate proteoglycan as a cell-surface endocytosis receptor. *Matrix Biol* 35, 51–55 <https://doi.org/10.1016/j.matbio.2013.10.004> PMID: 24145152
3. Neufeld E.F. and Muenzer J. (2001) The Mucopolysaccharidoses. In: Scriver CR, Beaudet A.L., Sly W. S., Valle D. editors. *The metabolic and molecular bases of inherited disease*, 8th ed. New York: McGraw-Hill. 3421–3452
4. Andrade F., Aldamzi-Echevarria L., Liarena M. and Couce M.L. (2015) Sanfilippo syndrome: Overall review. *Pediatr Int* 57(3), 331–338 <https://doi.org/10.1111/ped.12636> PMID: 25851924
5. Yogalingam G. and Hopwood J.J. (2001) Molecular genetics of mucopolysaccharidosis type IIIA and IIIB: Diagnostic, clinical and biological implications. *Hum Mutat.* 18(4), 264–281 <https://doi.org/10.1002/humu.1189> PMID: 11668611
6. Li H.H., Zhao H.Z., Neufeld E.F., Cai Y. and Gomez-Pinilla F. (2002) Attenuated plasticity in neurons and astrocytes in the mouse model of Sanfilippo syndrome type B. *J Neurosci Res* 69(1), 30–38 <https://doi.org/10.1002/jnr.10278> PMID: 12111813
7. Ohmi K., Kudo L.C., Ryazantsev S., Zhao H.Z., Karsten S.L and Neufeld E.F. (2009) Sanfilippo syndrome type B, a lysosomal storage disease, is also a tauopathy. *Proc Natl Acad Sci U.S.A.* 106(20), 8332–8337 <https://doi.org/10.1073/pnas.0903223106> PMID: 19416848
8. Ohmi K., Greenberg D.S., Rajavel K.S., Ryazantsev S., Li H.H. and Neufeld E.F. (2003) Activated microglia in cortex of mouse models of mucopolysaccharidoses 1 and IIIB. *Proc Natl Acad Sci USA* 100(4), 1902–1907. <https://doi.org/10.1073/pnas.252784899> PMID: 12576554
9. Archer L.D., Langford-Smith K.J., Bigger B.W., and Fildes J.E., (2014) Mucopolysaccharide diseases: a complex interplay between neuroinflammation, microglial activation and adaptive immunity. *J. Inherit Metab Dis* 1, 1–12.
10. Yogalingam G., Weber B., Meehan J., Rogers J. and Hopwood J.J. (2000) Mucopolysaccharidosis type IIIB: characterization and expression of wild-type and mutant recombinant alpha-N-acetylglucosaminidase and relationship with sanfilippo phenotype in an attenuated patient. *Biochim Biophys Acta* 1502 (3), 415–425. PMID: 11068184
11. Yogalingam G., Hopwood J.J., Crawley A. and Anson D.A. (1998) Mild feline mucopolysaccharidosis type VI. Identification of an N-acetylgalactosamine-4-sulfatase mutation causing instability and increased specific activity. *J Biol Chem* 273(22), 13421–13429. PMID: 9593674
12. Crawley A.C., Yogalingam G., Muller V.J. and Hopwood J.J. (1998) Two mutations within a feline mucopolysaccharidosis type VI colony cause three different clinical phenotypes. *J Clin Invest* 101(1), 109–119. <https://doi.org/10.1172/JCI935> PMID: 9421472
13. Clark W.T., Yu G.K., Aoyagi-Scharber M. and LeBowitz J.H. (2018) Utilizing ExAC to assess the hidden contribution of variants of unknown significance to Sanfilippo Type B incidence. *PLoS One* 13(7), 1–20
14. Conzelmann E. and Sandhoff K. (1983–1984) Partial enzyme deficiencies: residual activities and the development of neurological disorders. *Dev Neurosci* 6(1), 58–71.

15. Poswar F., Baldo G. and Giugliani R. (2017) 12, 1331–1340 Phase I and II clinical trials for the mucopolysaccharidoses. *Expert Opin Investig Drugs* 26(12), 1331–1340.
16. Kornfeld S. (1992) Structure and function of the mannose-6-phosphate/insulin-like growth factor II receptors. *Annu Rev Biochem*. 61, 307–30 <https://doi.org/10.1146/annurev.bi.61.070192.001515> PMID: 1323236
17. Zhao K.W. and Neufeld E.F. (2000) Purification and characterization of recombinant human alpha-N-acetylglucosaminidase secreted by Chinese hamster ovary cells. *Protein Expr Purif* 19(1), 202–211 <https://doi.org/10.1006/prep.2000.1230> PMID: 10833408
18. LeBowitz J.H., Grubb J.H., Maga J.A., Schmiel D.H., Vogler C. and Sly W.S. (2004) Glycosylation-independent targeting enhances enzyme delivery to lysosomes and decreases storage in mucopolysaccharidosis type VII mice. *Proc Natl Acad Sci USA* 101(9), 3083–3088 <https://doi.org/10.1073/pnas.0308728100> PMID: 14976248
19. Maga J.A., Zhou J., Kambampati R., Peng S., Wang X., Bohnsack R.N., Thomm A., Golata S., Tom P., Dahms N.M., Byrne B.J. and LeBowitz J.H. (2013) Glycosylation-independent lysosomal targeting of acid alpha-glucosidase enhances muscle glycogen clearance in pompe mice. *J Biol Chem* 288(3), 1428–1438 <https://doi.org/10.1074/jbc.M112.438663> PMID: 23188827
20. Kan S.H., Aoyagi-Scharber M., Le S.Q., Vincelette J., Ohmi K., Bullens S., Wendt D.J., Christianson T.M., Tiger P.M., Brown J.R., Yip B.K., Holtzinger J., Crippen-Harmon D., Vondrak K.N., Chen Z., Hague C.M., Woloszynek J.C., Cheung D.S., Webster K.A., Adintori E.G., Lo M.J., Wong W., Fitzpatrick P.A., LeBowitz J.H., Crawford B.E., Bunting S., Dickson P.I., Neufeld E.F. (2014). Delivery of an enzyme-IGFII fusion protein to the mouse brain is therapeutic for mucopolysaccharidosis type IIIB. *Proc Natl Acad Sci USA* 111(41), 14870–14875 <https://doi.org/10.1073/pnas.1416660111> PMID: 25267636
21. Aoyagi-Scharber M., Crippen-Harmon D., Lawrence R., Vincelette J., Yogalingam G., Prill H., Yip B.K., Baridon B., Vitelli C., Lee A., Gorostiza O., Adintori E.G., Minto W.C., Van Vleet J.L., Yates B., Rigney S., Christianson T.M., Tiger P.M.N., Lo M.J., Holtzinger J., Fitzpatrick P.A., LeBowitz J.H., Bullens S., Crawford B.E. and Bunting S. (2017) Clearance of Heparan Sulfate and Attenuation of CNS Pathology by Intracerebroventricular BMN 250 in Sanfilippo Type B Mice. *Mol Ther Methods Clin Dev* 6, 43–53 <https://doi.org/10.1016/j.omtm.2017.05.009> PMID: 28664165
22. Ellinwood N.M., Valentine B., Hess A.S., Jens J.K., Snella E.M., Ware W.A., Hostetter S.J., Ben-Shlomo G., Jeffery N., Safayi S., Smith J.D., Millman S.T., Parsons R.L., Butt M.T., Cooper J.D., Nesrasil vi., Prill H., i X., Zhou H., Lawrence R., Crawford B., Grover A., Melton A., Cherukuri A., Wait J.C. M., Pinkstaff J. and McCullagh E. (2018) Pharmacology of BMN 250 administered via intracerebroventricular infusion once every 2 weeks for twenty-six weeks or longer in a canine model of mucopolysaccharidosis type IIIB. *Mol Gen Metab* 123 (2), S42
23. Prill, H. et al., Rapid and efficient in-vitro uptake and lysosomal targeting of BMN 250 (NAGLU-IGF2) in primary cortical neurons and astrocytes under limited exposure conditions results in greater reduction of heparin sulfate storage than unmodified NAGLU in a cellular model of Sanfilippo B. In Preparation
24. Lawrence R., Olsen S.K., Steele R.E., Wang L., Warrior R., Cummings R.D., Esko J.D. (2008) Evolutionary differences in glycosaminoglycan fine structure detected by quantitative glycan reductive isotope labeling. *J Biol Chem* 283(48), 33674–84 <https://doi.org/10.1074/jbc.M804288200> PMID: 18818196
25. Lawrence R. Brown J.R., Al-Mafraji-K., Lamanna W.C., Beitel J.R., Boons G.J., Esko J.D., Crawford B. R. (2012) Disease-specific non-reducing end carbohydrate biomarkers for mucopolysaccharidoses *Nat Chem Biol* 8(2), 197–204. <https://doi.org/10.1038/nchembio.766> PMID: 22231271